

# Approximating the Quantum Approximate Optimisation Algorithm

David Headley,<sup>1,2,\*</sup> Thorge Müller,<sup>3,2,†</sup> Ana Martin,<sup>4</sup> Enrique Solano,<sup>4,5,6</sup> Mikel Sanz,<sup>4</sup> and Frank K. Wilhelm<sup>2</sup>

<sup>1</sup>*Mercedes-Benz AG, Stuttgart, Germany*

<sup>2</sup>*Theoretical Physics, Saarland University, 66123 Saarbrücken, Germany*

<sup>3</sup>*German Aerospace Center (DLR), 51147 Cologne, Germany*

<sup>4</sup>*Department of Physical Chemistry, University of the Basque Country UPV/EHU, Apartado 644, 48080 Bilbao, Spain*

<sup>5</sup>*IKERBASQUE, Basque Foundation for Science, Maria Diaz de Haro 3, 48013 Bilbao, Spain*

<sup>6</sup>*International Center of Quantum Artificial Intelligence for Science and Technology (QuArtist) and Department of Physics, Shanghai University, 200444 Shanghai, China*

(Dated: December 21, 2024)

The Quantum Approximate Optimisation Algorithm was proposed as a heuristic method for solving combinatorial optimisation problems on near-term quantum computers and may be among the first algorithms to perform useful computations in the post-supremacy, noisy, intermediate scale era of quantum computing. In this work, we exploit the recently proposed digital-analog quantum computation paradigm, in which the versatility of programmable universal quantum computers and the error resilience of quantum simulators are combined to improve platforms for quantum computation. We show that the digital-analog paradigm is suited to the variational quantum approximate optimisation algorithm, due to its inherent resilience against coherent errors, by performing large-scale simulations and providing analytical bounds for its performance in devices with finite single-qubit operation times. We observe regimes of single-qubit operation speed in which the considered variational algorithm provides a significant improvement over non-variational counterparts.

## I. INTRODUCTION

Quantum computing is entering an era in which classical computers cannot simulate the behaviour of programmable quantum computers [1]. In this new era of quantum information processing, it is likely that the first algorithms that will be useful for solving computational problems will be *heuristic* in nature. These algorithms come without provable performance guarantees provided by the likes of Shor’s factoring algorithm [2] or the Grover search algorithm [3], but are encouraged by strong motivation from classical algorithm research, in that the most effective algorithms for solving certain problems classically are often not provably so. At present, there are two such algorithms that are most likely to prove useful in the near term [4]—The Variational Quantum Eigensolver (VQE) [5] and the Quantum Approximate Optimisation Algorithm (QAOA) [6] otherwise known as the Quantum Alternating Operator Ansatz [7]. These are *variational* algorithms, using classical optimisers and parameterised quantum circuits to mitigate the effects that errors may introduce on quantum devices making no use of quantum error correction. This work concerns the latter of the two.

QAOA is a discrete-time hybrid quantum-classical algorithm for computing solutions to problems in combinatorial optimisation. The algorithm was initially discovered to provide greater approximation ratios than the best known classical algorithm for the problem type MAX-E3LIN2 [8], a result later ceded to a quantum-inspired classical algorithm [9]. It was demonstrated

by Jiang et al. [10] that QAOA can recover the square root scaling of the Grover’s search algorithm, replicating Grover’s speed-up without the need for Grover’s mixing operator. Hadfield et al. discovered that QAOA driving operators can be modified such that a wide variety of problems can be solved without resorting to high-order penalty-terms usually considered in an annealing or adiabatic-based approach [7].

The development of QAOA was motivated by a need for algorithms that can run on noisy, pre-error correction devices. Algorithms used on devices of this era will necessarily have a degree of co-design between architecture and algorithm. Work by Rigetti, for example, used a noisy, programmable quantum device to solve a combinatorial optimisation problem inspired by the on-device layout of qubits [11]. Following this approach, we extend the work of Parra-Rodriguez et al. on the Digital Analog (DA) paradigm of quantum computation [12–14], in which a device is designed and operated in the style of a *quantum simulator* with always-on multi-qubit interactions. We show that QAOA is a natural algorithm for this setting. This paradigm, leveraged to minimise errors associated with turning on and off gates on a quantum device, could allow for a simpler design in which only the timing of single-qubit gates must be considered, reducing the control complexity and, therefore, the mechanisms through which environmental noise can corrupt the computing system.

## II. THE DIGITAL-ANALOG QUANTUM COMPUTATIONAL PARADIGM

Quantum algorithms can, in general, be separated into two time classes: continuous and discrete. At the ex-

\* David.Headley@daimler.com

† Thorge.Mueller@dlr.de

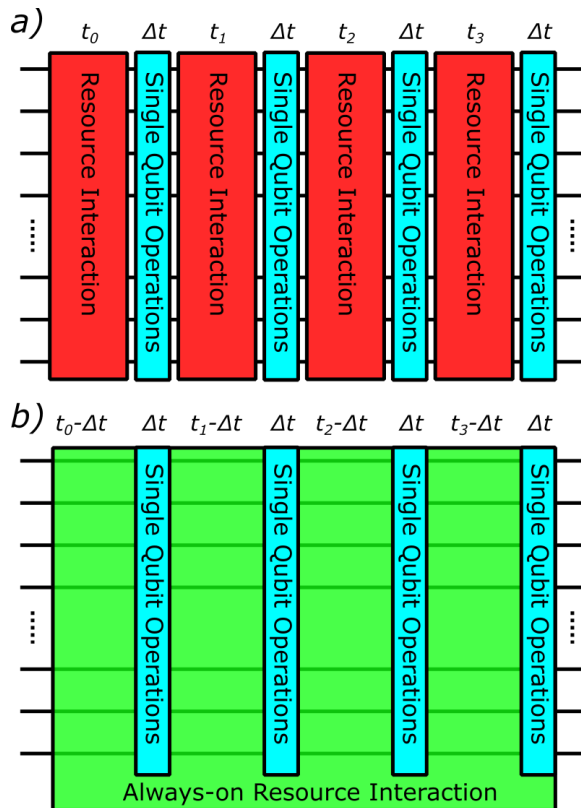


FIG. 1. The two schemes for digital analog computation. a) The stepwise or sDAQC scheme in which a series of programmable *digital* single qubit gates are applied in alternation with *analog* resource interactions. b) The always-on or bDAQC scheme in which the resource interaction is never turned off and single qubit operations are applied in parallel with the resource interactions. Performing the single qubit operations simultaneously with the resource interaction introduces coherent errors but reduces device control requirements. The first interaction block denoted with the time interval  $t_0$  corresponds to the *idle* block.

Extreme end of continuous quantum algorithms lie quantum simulators, devices fabricated to follow dynamics of interest with, however, no capacity for complicated programmed time evolution [15]. Likewise, continuous algorithms such as the quantum adiabatic algorithm [16, 17] and quantum random walk algorithms [18, 19] make use of a predefined *analog* Hamiltonian with generally limited programmability to solve computational problems. Discrete algorithms, on the other hand, are defined in terms of sequences of *digital* unitary gates. A gate-based quantum computer can perform any discrete, gate-based algorithm, including Trotterized versions of continuous algorithms [20]. Whereas, a device designed for continuous quantum algorithms, though may be theoretically universal, will generally only be able to run the restricted set of time evolutions for which they are built—it is in theory possible to express any discrete time quantum algorithm (e.g. Shor’s) as a continuous time quantum algorithm, but generally not practical [21].

The DA paradigm [12, 13] is a scheme designed to take the best features of both digital and analog quantum computing and has been recently demonstrated to yield an implementation for the quantum Fourier transform, in which significant advantages over regular digital schemes are demonstrated for reasonable coherent-control error assumptions [14]. Digital Quantum Computing (DQC) allows flexibility for a device to carry out any task compiled to the device’s native gates, whereas analog quantum computation, i.e. quantum simulators, benefit from superior noise resilience characteristics stemming from reduced requirement to completely control the full dynamics of every qubit [22]. The basic premise of the DA scheme is that blocks resembling the time evolution of an analog simulator are performed, punctuated by digital single-qubit operations. This is depicted in quantum circuit form in Fig. 1. The DA paradigm comes in two varieties, the *step-wise* scheme (sDAQC) and the *always-on* or *banded* scheme (bDAQC) which introduces error to computations due to the non-commutativity of single qubit operations used in conjunction with an entangling resource interaction. This work proposes the use of always-on- or bDAQC-QAOA on near-term devices for quantum optimisation, for which the step-wise scheme provides a guarantee that in the limit of infinitely fast single-qubit operations, bDAQC-QAOA is identical to error-free QAOA.

Following the work of Parra-Rodriguez et al. [13], we consider a context in which we take access to a *resource* Hamiltonian consisting of a sum of all interaction terms between connected qubit pairs on an  $n$ -qubit device. We use this resource as an entangling operation to simulate problem Hamiltonians required for QAOA. In sDAQC we assume that our device has the capability for this resource Hamiltonian to be turned on and off, alongside the ability to perform arbitrary single-qubit gates. We can therefore alternate blocks of our resource interaction with digital blocks of single-qubit gates. In bDAQC we do not make use of the controllability of the resource Hamiltonian, but retain the ability to perform arbitrary single-qubit gates at any time. Let us assume that the resource Hamiltonian available is an all-to-all (ATA) Ising Hamiltonian:

$$H_{\text{Resource}} = \sum_{j < k}^n r_{jk} Z_j Z_k, \quad (1)$$

where in the *homogeneous* case,  $r_{jk} = 1 \forall j, k$  (the units of  $r$  are set such that 1 represents a relevant energy scale for the device). All sums over qubit indices start from 1. In the simulations and resource estimates performed in this work, we consider only resource Hamiltonians in which no element of  $r$  is zero. However, the following procedure does not require an all-to-all connected resource interaction to succeed. Here, we require only that the interactions present in the arbitrary Hamiltonian that we intend to simulate are also non-zero in the resource Hamiltonian. Although this is not necessary in general [23], we assume it for the sake of simplicity. This resource

can be used to simulate the unitary evolution generated by any arbitrary spin glass Hamiltonian. Experimental settings likely to provide such resource Hamiltonians are discussed in section VI.

The procedure to determine a sequence of single-qubit rotations intersperses single-qubit- $X$  operations around analog blocks to *steer* the resource Hamiltonian to effect an arbitrary Ising Hamiltonian. There are  $2^{2n}$  possible manners in which  $n$ -qubit blocks could be surrounded by  $X$  rotations but, following Ref. [13], only blocks surrounded symmetrically by two single-qubit- $X$  operations are considered in our procedure. Of these single-qubit- $X$  operators there will often be cancellations between layers, reducing the total number of single-qubit gates required. We want to simulate the Hamiltonian  $H_{\text{Arb}}$  to effect the unitary  $U_{\text{Arb}}$ , respectively defined by

$$U_{\text{Arb}}(t) = e^{iH_{\text{Arb}}t} \quad \text{and} \quad H_{\text{Arb}} = \sum_{j < k}^n g_{jk} Z_j Z_k, \quad (2)$$

which we want to express in the form:

$$H_{\text{Arb}} = \sum_{j < k}^n \sum_{l < m}^n t_{lm} r_{jk} X_l X_m Z_j Z_k X_l X_m, \quad (3)$$

for some time vector  $\vec{t}$  that we wish to compute. This expression can be manipulated to the form:

$$\sum_{j < k}^n \sum_{l < m}^n t_{lm} r_{jk} (-1)^{\delta_{lj} + \delta_{lk} + \delta_{mj} + \delta_{mk}} Z_j Z_k \quad (4)$$

using the identity  $XZ \equiv -ZX$  to commute the Pauli- $X$  operators to cancellation. Through this expression we replace  $n(n-1)/2$  possible interaction strengths  $g_{jk}$  between qubits  $j, k$  with  $n(n-1)/2$  resource interaction times  $t_{lm}$  sandwiched by single-qubit- $X$  operators on qubits  $l, m$ . The Hamiltonian in equation (3) is easily implementable on a quantum computer with single-qubit- $X$  and time evolution with  $ZZ$  interactions due to the expression

$$e^{itUVU^\dagger} = \sum_{k=0}^{\infty} \frac{(it)^k (UVU^\dagger)^k}{k!} = U e^{itV} U^\dagger \quad (5)$$

valid for any unitary operator  $U$ . Using the linear independence of Pauli strings, we can write

$$\frac{g_{jk}}{r_{jk}} = \sum_{l < m}^n t_{lm} (-1)^{\delta_{lj} + \delta_{lk} + \delta_{mj} + \delta_{mk}} \quad (6)$$

in which finding  $g_{jk}$  is a matrix inversion problem made apparent by consolidating the parameter pairs  $l, m$  and  $j, k$  each to one parameter

$$\kappa = n(l-1) - \frac{l(l+1)}{2} + m, \quad (7)$$

$$\mu = n(j-1) - \frac{j(j+1)}{2} + k. \quad (8)$$

We arrive at a solution in time scaling at most  $O(n^6)$  using Gaussian elimination on a classical computer of a matrix with dimension  $n(n-1)/2 \times n(n-1)/2$  of

$$t_\kappa = M_{\kappa\mu}^{-1} (g/r)_\mu \quad \text{for} \quad M_{\kappa\mu} = (-1)^{\delta_{lj} + \delta_{lk} + \delta_{mj} + \delta_{mk}}. \quad (9)$$

$M$  has been shown to be non-singular in the case that  $n \neq 4$  but an alternative procedure can be followed in this case [13]. QAOA problems of interest, however, far exceed this value in size. An obstacle for the usage of this scheme is that any of the times calculated in this procedure may be negative. Following the computation of a time vector  $t_\kappa$  providing a DA circuit to simulate a desired Ising Hamiltonian, negative times must be eliminated as it is experimentally impossible to run an always-on interaction—the nature of which we can't temporarily change—for a negative time.

Here, we present a procedure that exploits the case in which the resource Hamiltonian is homogeneous, or one of  $\vec{g}, \vec{r}$  takes only values with some least common multiple, resulting in periodic time-evolution. This condition holds for MAX-CUT and SAT problems considered in this work (all  $ZZ$  Hamiltonian terms in section IV have at least half-integer pre-factors). In the case that the resource Hamiltonian is homogeneous, any negative time-block can simply be run for a positive time, exploiting the periodicity of the unitary effected as  $e^{iHt} = e^{iH(2\pi+t)}$ , for  $r_{jk} = 1 \forall j, k$ . As such, with homogeneous resource Hamiltonians we can always replace  $t_{lm}$  with  $t_{lm} \bmod 2\pi$ . This technique, involving a homogeneous resource, is unfortunately undesirable as a method to rectify all negative time blocks as we will take a time interval that is typically small and replace it with a larger time  $2\pi - |t_{lm}|$ . This will result in an DA schedule of single-qubit gates and analog block times requiring an impractically long total time to run on hardware.

For an inhomogeneous resource Hamiltonian we need to consider one additional time-block surrounded by no single-qubit operations. To determine the size of this *idle* block required, consider

$$M\vec{t} = M(\vec{t} - t_{\min}\vec{1} + t_{\min}\vec{1}). \quad (10)$$

$M$  admits  $\vec{1}$  as an eigenvector with eigenvalue  $\lambda$ . Intuitively,  $\vec{1}$  is an eigenvector of  $M$  because when applying all possible two- $X$ -surrounded DA blocks for an equal time, the time evolutions mostly cancel out leaving a smaller but homogeneous effective interaction. This produces

$$M\vec{t} = M(\vec{t} - t_{\min}\vec{1}) + \lambda t_{\min}\vec{1} \quad (11)$$

and considering a new, non-negative time vector  $\vec{t}^* = \vec{t} - t_{\min}\vec{1}$

$$M\vec{t} = M\vec{t}^* + \lambda t_{\min}\vec{1}. \quad (12)$$

Applying all possible two-qubit- $X$  DA blocks does not, however, result in a similar homogeneous contribution to the simulated Hamiltonian to resource Hamiltonian ratio for all system sizes. We wish to have an eigenvalue  $\lambda$

that is negative, such that when multiplied by negative  $t_{\min}$  we produce a positive idle time. Unfortunately, the contributions to the ratio for NISQ-relevant cases with  $n > 7$  are, themselves, positive. The relation between  $n(n+1)/2 + 1$  time-intervals and the Hamiltonian simulated can be written as

$$g_{\kappa} = M_{\kappa\mu} t_{\mu}^* r_{\kappa} + t_{\text{idle}} r_{\kappa} \quad (13)$$

with  $t_{\text{idle}} = \lambda t_{\min}$ . We solve the negativity problem by letting the always-on resource Hamiltonian run for time  $\lambda t_{\min}$  surrounded by no single-qubit gates if  $t_{\min}$  is negative. Since  $t_{\text{idle}}$  is negative for relevant cases of  $n > 6$ , we must use one of two methods to change the sign of this time, depending on whether a homogeneous or inhomogeneous resource Hamiltonian is available. If the resource is homogeneous we can evolve for time  $t_{\text{idle}} \bmod 2\pi$ , as before. This cost of running for this positive time will only add a small contribution to the total algorithm run-time since it only occurs once per DA block. In realistic experimental cases, however, we expect only non-homogeneous resource Hamiltonians to be available. Even with non-homogeneous resource Hamiltonians, non-negative idle time is still possible through exploiting properties of the simulated problem Hamiltonian. By setting  $H_{\text{Arb}} \rightarrow -H_{\text{Arb}}$  in equation (2) and using the fact that all  $ZZ$  coupling constants in  $H_{\text{Arb}}$  will be integer multiples of  $1/2$  or zero for MAX-CUT and MAX-2-SAT problems, we can simulate the Hamiltonian of correct sign by exploiting the periodicity of the unitary effected, as  $e^{itH_{\text{Problem}}} = e^{i(-t)(-H_{\text{Problem}})} = e^{i(-t \bmod 2\pi)(-H_{\text{Problem}})}$ . This factor of  $-1$  in front of the problem Hamiltonian can then be absorbed into the matrix  $M$  in equation (13) causing the eigenvalue  $\lambda$  to become negative. This allows a positive idle-time correction, resolving the negative sign issue for inhomogeneous cases.

The method presented here provides a convenient decomposition of an arbitrary Ising Hamiltonian into time-blocks of our resource interaction surrounded by two pairs of single-qubit rotations. The problem of negative times is resolved for the case of resource or target Hamiltonians satisfying certain constraints. For Hamiltonians not satisfying the aforementioned constraints, approaches including the decomposition into multiple DA sequences satisfying these constraints, or a strategy involving a higher number of analog blocks could still be pursued. To incorporate a greater number of time blocks one could solve the under-determined linear system  $\vec{g} = M\vec{t}$  with  $\vec{t} \geq 0$  where the time-vector  $\vec{t}$  is of higher dimension than  $\vec{g}$  and, therefore,  $M$  is no longer square (and invertible). Approaches to solve such a problem are complicated by the time non-negativity constraints and require a quadratic programming approach. Recent work by Galicia et al. [23] extends the digital-analog paradigm to the scenario in which only interactions available on a device with linear, nearest-neighbour connectivity can be used to systematically produce an all-to-all connected arbitrary Hamiltonian. Strategies for architectures that

are more connected than linear, yet not fully connected, can therefore also produce arbitrary Ising Hamiltonians, by restriction to a linear chain, or by manually inserting the SWAP operations of a SWAP network [24], themselves compiled to digital-analog sequences.

### III. THE QUANTUM APPROXIMATE OPTIMISATION ALGORITHM

The Quantum Approximate Optimisation Algorithm is a hybrid quantum classical algorithm in which a classical optimiser tunes the  $2p$  parameters  $\vec{\gamma}, \vec{\beta}$  of a quantum circuit to maximise an objective function corresponding to high-quality solutions of a combinatorial optimisation problem. In QAOA, an ansatz state

$$|\vec{\beta}, \vec{\gamma}\rangle = \prod_{p'=1}^p e^{i\beta_{p'} H_D} e^{i\gamma_{p'} H_P} |+\rangle^{\otimes n} \quad (14)$$

is generated on a quantum processor using  $p$  repetitions of two Hamiltonians—a problem Hamiltonian  $H_P$  and a driver Hamiltonian  $H_D$ —for which a quantum circuit can be seen in Fig. 2.  $H_P$  is a Hamiltonian defined by a combinatorial optimisation problem instance that we intend to solve with

$$H_P = \sum_{z=0}^{2^n-1} C(z) |z\rangle \langle z| \quad (15)$$

where  $C$  is the value of the optimisation problem's objective function taking input strings  $z$ . The driver Hamiltonian in QAOA takes the usual form of

$$H_D = \sum_{i=1}^n X_i \quad (16)$$

and is chosen for its ease of implementation as a non-interacting Hamiltonian, whilst still facilitating population transfer between any two given states.

To solve a problem with QAOA, the QAOA circuit is run a number of times and the output string measured to calculate an expectation value of  $H_P$  under the QAOA ansatz state for the current parameters

$$\langle H_P \rangle_{\vec{\beta}, \vec{\gamma}} = \langle \vec{\beta}, \vec{\gamma} | H_P | \vec{\beta}, \vec{\gamma} \rangle \quad (17)$$

as in figure 2. With or without some post processing [25] this value is handed to a classical optimiser with the aim of producing new parameters via a classical black box optimisation strategy. The expectation value of the problem Hamiltonian is computed again and the process is repeated for either a fixed amount of time or until a satisfactory solution to the problem is discovered. A flowchart depiction of this process is demonstrated in figure 3. Problem-independent success in QAOA is measured in terms of the *mean approximation ratio* defined

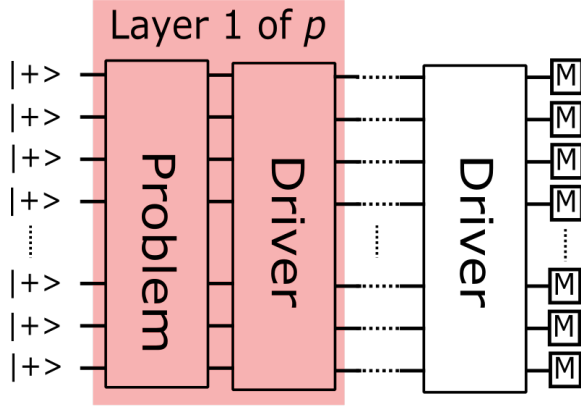


FIG. 2. A typical QAOA state preparation circuit. A problem and driver Hamiltonian are alternated  $p$  times, applied to the  $|+\rangle^n$  state, followed by measurement on all qubits.

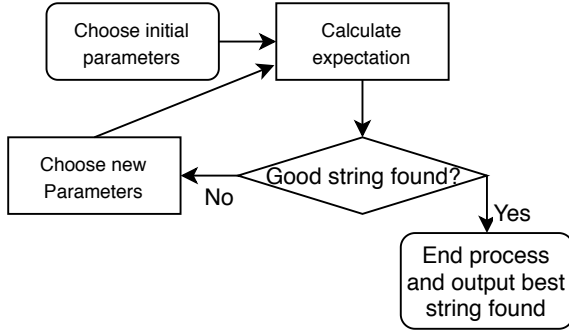


FIG. 3. The process followed in QAOA. A loop of calculating expectation values and changing parameters is run until a satisfactory string is found.

by:

$$\frac{\langle H_P \rangle_{\vec{\beta}, \vec{\gamma}}}{\|H_P\|}. \quad (18)$$

Combinatorial optimisation problems with clauses encompassing at most two bits can be expressed in terms of two-qubit  $ZZ$  interactions and single-qubit- $Z$  rotations. Problems in which the clauses are local to more bits require higher order terms and are therefore generally out of reach of NISQ quantum computers. Two problems discussed in the literature that do not concern terms of order higher than 2 are the problems of MAX-CUT and MAX-2-SAT. MAX-CUT, defined on a problem graph in which

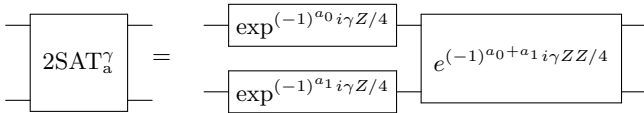


FIG. 4. Circuit showing the decomposition of a SAT-clause problem Hamiltonian using only  $Z$ -type operators.  $a$  describes the type of the SAT clause with  $a = 0$  being an OR clause between un-negated variables.

each vertex is a binary variable, is a problem in which the objective is to find the graph partition such that the number of edges crossing said partition is maximised. The clauses of the problem, or edges of the problem graph are of the type XOR between problem variables. XOR admits the truth table  $00, 01, 10, 11 \rightarrow 0, 1, 1, 0$  which can be decomposed into a  $Z$ -based Hamiltonian following theorem 10 of Ref. [26]. A MAX-CUT clause, therefore, manifests in the problem Hamiltonian as

$$H_{C,jk} = \frac{1}{2} (I - Z_j Z_k) = \text{diag}(0, 1, 1, 0). \quad (19)$$

The identity in this expression has no effect other than to keep the Hamiltonian non-negative such that the diagonal corresponds to the number of edges a given allocation cuts.

In recent literature, the problems of 2- and 3-SAT have seen significant attention due to the presence of *reachability deficits* [27] in the depth of QAOA required to find an optimal solution. MAX-2-SAT encompasses a more general set of problems than MAX-CUT, as MAX-CUT problems form a subset of possible MAX-2-SAT problems. Two 2-SAT clauses can be combined to construct a CUT clause but a 2-SAT clause cannot be constructed from multiple CUT clauses. A 2-SAT clause between two bits can take four forms:  $(b_1 \vee b_2)$ ,  $(b_1 \vee \neg b_2)$ ,  $(\neg b_1 \vee b_2)$ ,  $(\neg b_1 \vee \neg b_2)$ . The logical OR operation  $\vee$  yields a truth table  $00, 01, 10, 11 \rightarrow 0, 1, 1, 1$  that we can express as a diagonal Hamiltonian  $\text{diag}(0, 1, 1, 1) = I - |\vec{0}\rangle\langle\vec{0}|$ . Using the same procedure as before, the four 2-SAT clause types have problem Hamiltonians on the two constituent qubits of

$$H_{\vec{a}} = I - |\vec{a}\rangle\langle\vec{a}| \quad (20)$$

which yields a  $Z$  operator decomposition as

$$H_{\vec{a}} = I - \frac{1}{4} [I + (-1)^{a_0} Z_0 + (-1)^{a_1} Z_1 + (-1)^{a_0+a_1} Z_0 Z_1] \quad (21)$$

where  $\vec{a}$  is a binary vector denoting which of the four clause types is used. Figure 4 shows this decomposition in circuit form.

Both MAX-CUT and MAX-2-SAT are NP-complete problems [28], meaning that any other NP-complete problem may be reduced to these problems. Such reductions, however, are unlikely to provide useful implementations on NISQ devices due to large polynomial increases in the number of clauses and variables required to express a reduced problem.

#### IV. DIGITAL ANALOG QAOA

In DA-QAOA we assume access to a device with the following Hamiltonian

$$H_{\text{Device}}(t) = f(t)H_{\text{resource}} + \alpha \sum_{i=1}^n (x_i(t)X_i + z_i(t)Z_i) \quad (22)$$

where

$$H_{\text{Resource}} = \sum_{j < k}^n r_{jk} Z_j Z_k. \quad (23)$$

In the stepwise scheme (sDA-QAOA), we assume control over the parameters  $f, x_i, z_i$  each taking values from  $\{0, 1\}$ . In the banged scheme (bDA-QAOA),  $f$  is always set to 1 and only the single-qubit parameters may be altered. The single qubit terms are stronger than the resource Hamiltonian by the factor  $\alpha \geq 1$  and in typical applications  $\alpha$  is expected to fall between 10 – 1000 depending on architecture [29, 30]. Though current devices tend to exhibit a ratio of single qubit rotation speed to interaction strength at the lower end of this range, they have little to gain from faster single-qubit operations, since they are typically limited by two-qubit interaction times and fidelity. We therefore expect that a device optimising for DA applications could be engineered for greatly higher ratios  $\alpha$ . During driving in bDAQC, all single-qubit- $X$  operations are set to 1,  $Z$  terms to 0, giving a driver Hamiltonian of

$$H_{\text{bDA-Driver}} = \sum_{j < k} r_{jk} Z_j Z_k + \alpha \sum_{i=0}^n X_i \quad (24)$$

applied for device time given by the variational parameter  $\beta$  divided by the driver strength  $\alpha$  with  $\beta \in [0, \pi]$ . During the DA resource Hamiltonian steering operations, we use a similar Hamiltonian in which only a specific set of single-qubit- $X$  terms are active. As described in section II, we wish to implement a full  $X$ -gate before and after each resource block. The time to apply this gate will be  $\Delta t = \frac{\pi}{\alpha}$ . Applying the DA-QAOA device Hamiltonian for a single QAOA layer thus effects the following unitary

$$U_{\text{DA-QAOA}} = \mathcal{T} \exp\left(-i \int_{t=0}^{t_{\text{total}}} H_{\text{Device}}(t) dt\right), \quad (25)$$

with  $\vec{x}(t)$  defined by the aforementioned matrix inversion procedure,  $\mathcal{T}$  is the time-ordering meta-operator and  $\vec{z}(t)$  used in the case that we are solving a SAT problem.  $t_{\text{total}}$  is the sum of all times in the non-negative DA time vector multiplied by the variational parameter  $\gamma$  in addition to the driving time  $\beta/\alpha$ . A depiction of this device Hamiltonian used to apply a MAX-CUT problem Hamiltonian is presented in Fig. 5.

## V. COMPILATION COSTS OF DA-QAOA

In this section the cost in on-device time to perform QAOA using DAQC and different resource Hamiltonians is evaluated. We include in our comparison the time taken by a completely digital quantum computer under reasonable assumptions. We emphasise here that the time taken to perform an algorithm is only a good indication of the fidelity of the algorithm's experimental

implementation (or quality of solution) if the device running the experiment is *coherence limited*. In contemporary quantum processors, the limitation is typically not coherence time but the error incurred during the use of two-qubit operations, per operation. An evaluation of whether a device using a DAQC or DQC paradigm performs better would require in-depth knowledge of the error mechanisms of a device operating in the respective paradigm. Such an analysis is expected to favour DAQC given the reduction of errors from turning couplings on and off.

When comparing the performance of a device making use of the DAQC paradigm to a device running completely digital computations, we must make fair assumptions concerning the capability of each device. We compare the case in which both DAQC and DQC can perform interactions between any pair of qubits. In DQC, the key limitation we apply—besides the differing error models that are expected to comprise the main advantage of DAQC—is the inability to perform simultaneous two-qubit gates on a single qubit. A given QAOA problem Hamiltonian in DQC must therefore be decomposed into a number of time-steps. This number of time steps for a graph-based problem can be shown to, at most, equal the maximum vertex degree of the problem graph plus one. DAQC in comparison, applies all operations at once, but must utilise many time-blocks to time-average the device resource interaction to the problem Hamiltonian of interest. An example of a QAOA MAX-CUT problem compiled to both the DQC and DAQC is found in figure 5 for a 5-regular MAX-CUT problem on a 8 qubit device. One notes that for this particular problem, the DA circuit can be performed faster than the digital for sufficiently fast  $X$  gates.

Comparisons of the time taken for to implement a problem Hamiltonian are presented in figure 6. In this plot we compare Hamiltonians from the hardware architectures section, with homogeneous and inhomogeneous resource interactions. For the inhomogeneous resource interactions, we use couplings  $r_{jk} \sim \mathcal{N}(1, \delta^2)$  where  $\delta$  is the fractional standard deviation of the coupling strength. Values of 5% and 10% are used for this inhomogeneity. For the  $|r|^{-6}$  and  $|r|^{-3}$  power law behaviour, we assume that qubits are placed on in a linear array. For a fair comparison between these resource Hamiltonian and the others, we scale the couplings such that the average coupling between two qubits is the same for all resource Hamiltonians used. Disregarding the speed advantage from exploiting the periodicity of a homogeneous resource, small deviations in the couplings do not greatly affect the compiled time. If, however, any individual coupling becomes especially small, the compilation time grows correspondingly large.

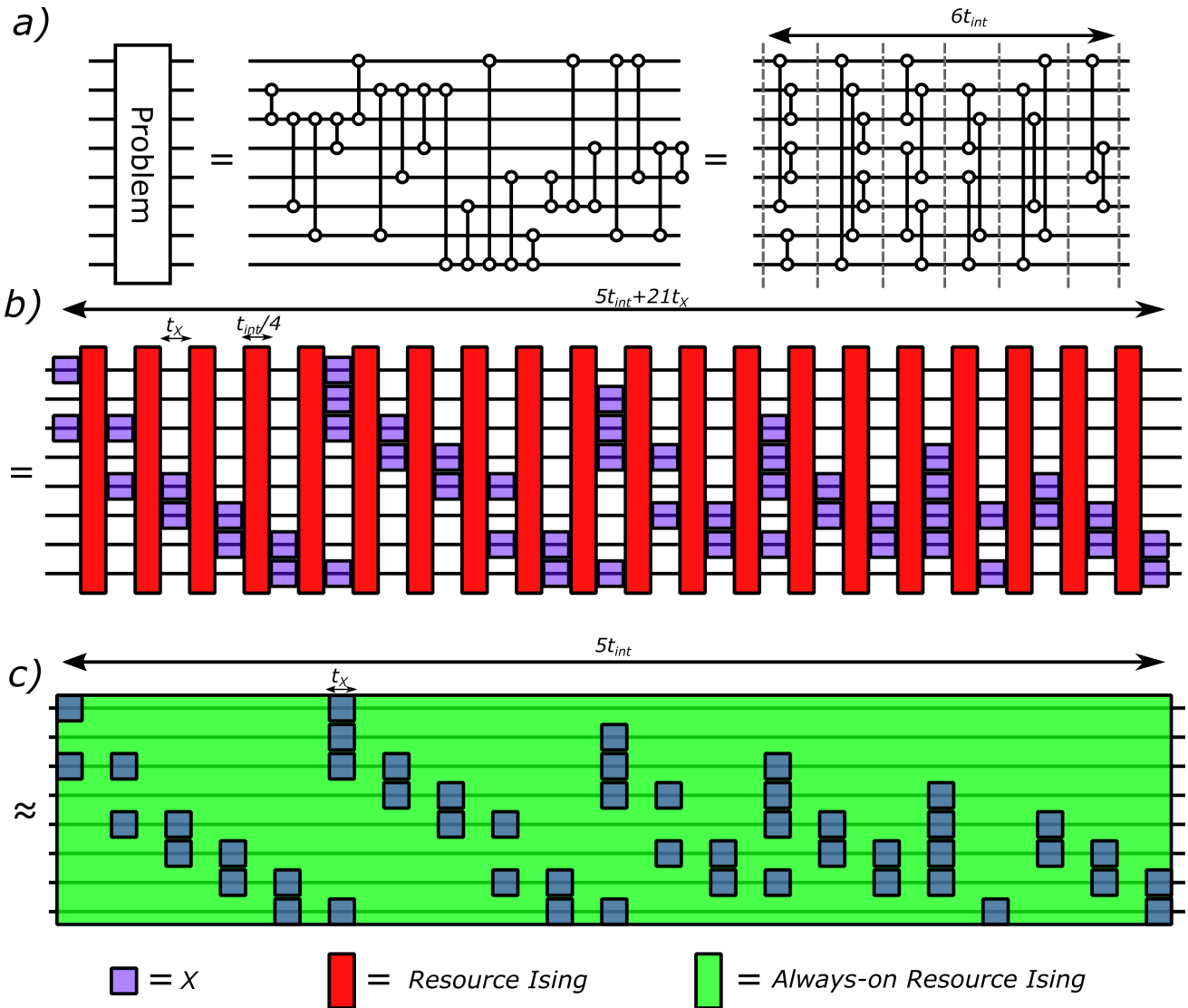


FIG. 5. Circuit compilations for an 8-qubit MAX-CUT problem on a 5-regular graph. a) A decomposition of the MAX-CUT problem Hamiltonian into  $ZZ$  interactions. The lines connected to two open circles represent  $ZZ$  interactions applied for time  $t_{int}$ . On the right hand side, we see that the circuit can be parallelised into six time-steps, each of which sees one qubit interact with only one other qubit at a time. Six time-steps corresponds to the maximum degree of a vertex plus one. b) The same circuit can be compiled into the scheme of bDAQC in which a resource all-to-all homogeneous Ising Hamiltonian is turned on and off, punctuated by single qubit gates. This decomposition requires 20 uses of the resource Hamiltonian and 50 single-qubit- $X$  operations. The time taken to apply the problem Hamiltonian is  $5t_{int} + 21t_x$ . c) Finally, we compile the problem Hamiltonian in the sDAQC scheme, in which the resource Hamiltonian remains on throughout the procedure. This circuit only approximates the time evolution invoked by the QAOA problem Hamiltonian but can be carried out in time  $5t_{int}$  and also with 49 single-qubit- $X$  operations. In the limit of infinitely fast  $X$  gates, c) is equivalent to a) and b).

## VI. HIGH-CONNECTIVITY NISQ HARDWARE PLATFORMS FOR DA-QAOA

A NISQ device able to solve a wide variety of combinatorial optimisation problems running QAOA would require a highly connected quantum device to avoid the need for swapping operations. One could then utilise platforms in which non-local interactions occur natively, while benefiting from the reduced control overhead provided by the digital analog scheme. It has been proposed

to use the digital analog scheme to compile SWAP gates themselves to sequences of digital and analog blocks [23]. For realistic near term hardware, however, we expect any algorithm utilising swap operations to be out of reach of near term hardware, whether compiled to digital gates or to digital analog time-blocks due to their excessive contribution to circuit depth and, therefore, decoherence.

Generally considered to be the most mature platform for quantum computing, superconducting solid state qubit architectures tend to have low connectivity due to

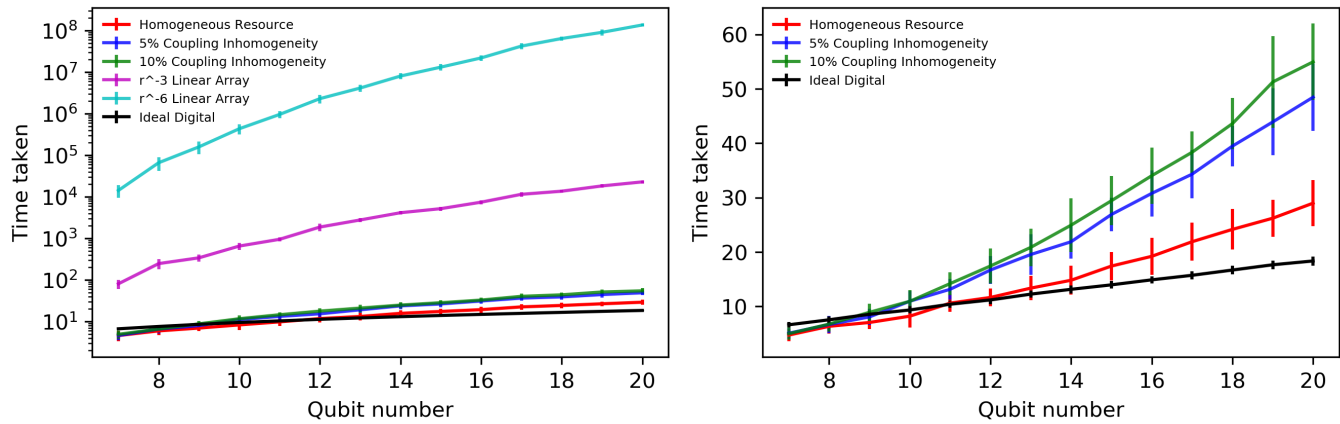


FIG. 6. Plots showing the on-device required time for implementation of a QAOA problem Hamiltonian. In this case random Erdős Rényi MAX-CUT problems are used with a filling factor of 0.75. Units of time are defined relative to the native device resource interaction strength. In these plots we show the time taken when using various possible resource Hamiltonians. The left hand side demonstrates that if the resource Hamiltonian available varies across orders of magnitude in coupling strength, as happens in the case of an inverse power law coupling between qubits in an array, the time taken in the digital analog scheme becomes extremely large (and likely impractical). The right plot shows the series in the left excluding the inverse power law couplings. A homogeneous resource Hamiltonian is competitive with an idealised digital compiling scheme, though higher for qubit numbers higher than 10. The upper blue and green lines demonstrate that if we use a resource Hamiltonian with normally distributed couplings close to 1 (standard deviations 0.05 and 0.1), the time taken is longer. The significant gap between the Homogeneous and non-homogeneous series occurs as the periodicity of the homogeneous resource Hamiltonian’s effected time evolution can be exploited to reduce the idle time.

their 2d-designed nature and are, in current manifestations, not an ideal candidate for performing DA-QAOA [31], though this direction could be explored in future work. Other systems, for example, Rydberg neutral atom arrays or cold, trapped-ion architectures allow for native interactions between all qubits in a device.

Rydberg neutral atoms are atoms in which one or more electrons are in a highly excited state. Excited states of these atoms have high lifetimes owing to their large spatial extent and, therefore, small spatial overlap with the ground state of the atom [32]. Optical lattices of Rydberg atoms can feature non-local, all-to-all Van-der-Waals interactions scaling with  $|1/r|^6$  for distances  $r$  greater than the optical lattice spacing. Such an interaction is highly non-homogeneous but could be utilised for the digital analog scheme.

Trapped ion systems have demonstrated the highest fidelity two-qubit operations [29, 33] and highest coherence time of any existing platform [34]. These systems, however, fail to achieve high-fidelity when many qubits are loaded into a trap. This limitation occurs due to frequency crowding of the energy levels used to address the coupling of each ion to the collective motional state of the trapped ions. When the requirement for control over interactions between individual ions in a trap is relaxed, trapped ion platforms perform exceptionally as simulators [35] and qubit numbers competitive with the best superconducting processors can be used to explore physics outside the reach of classical simulation. Interactions between trapped ions scale on the order of  $|1/r|^\delta$  with  $\delta$  typically varying between 0 – 3 [36], with  $r$  as the distance

between two trapped ions. A system utilising a value of  $\delta = 0$ —in which the interaction is mediated by the joint vibrational modes—would have a homogeneous coupling if no other non-homogeneous behaviour is present between pairs of ions. The case of  $\delta = 3$  occurs when the interaction is mediated purely via spin-spin interactions, incurring a dipolar decay law.

## VII. PERFORMANCE OF bDA-QAOA

In bDA-QAOA we perform QAOA using the ansatz state prepared by applying QAOA layers of the form described in equation (25) as

$$|\vec{\beta}, \vec{\gamma}\rangle^{\alpha, \text{DA}} = U_{\alpha, \text{DA-QAOA}} |+\rangle^{\otimes n}. \quad (26)$$

bDA-QAOA introduces errors in the form of the misspecification of the problem and driver Hamiltonians, between which, due to relative times taken on device to perform and that the driver is generic to all problems, the misspecification of problem Hamiltonian will introduce more error. This problem of misspecification is not new to the field of quantum optimisation and is known in quantum annealing literature as  $J$ -chaos, in which critical characteristics of a problem to be solved are not correctly incorporated into the dynamics of an annealing device. Such issues can be fatal to the performance of AQC if error mitigation strategies are not utilised [37]. bDA-QAOA finds connection to the algo-

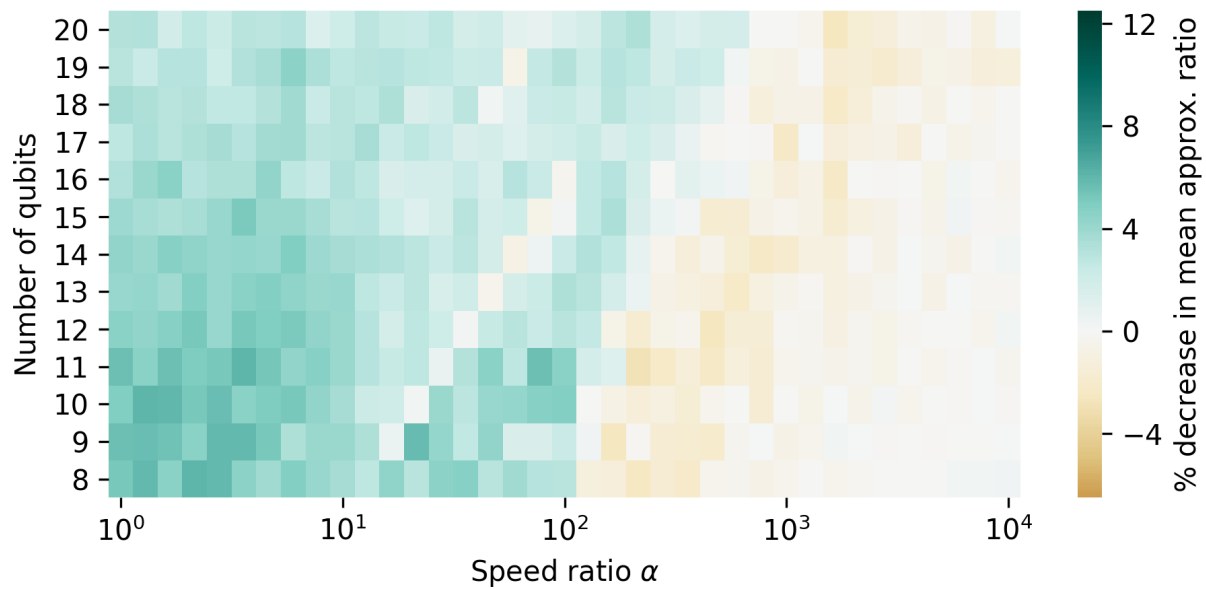


FIG. 7. The percentage difference between the mean approximation ratio attained by bDA-QAOA and error-free QAOA, averaged over 50 randomly generated MAX-CUT problems with constant filling factor  $p_{\text{clause}} = 0.7$ . Blue colours indicate that the bDA-QAOA ansatz state is worse than that provided by error-free QAOA, whereas, shades of brown indicate an improvement of the bDAQC over error free QAOA. On the  $x$ -axis, the ratio  $\alpha$  of single-qubit to problem Hamiltonian term strength is seen where error-free QAOA exists in the limit as this ratio becomes infinite.

gorithms of QRW [38] and AQC in that the problem Hamiltonian and single-qubit driving operators are performed simultaneously. One might therefore expect that simply running a problem Hamiltonian at the same time as a driver in QAOA should not be fatal, in fact, scheduled QRW's and diabatic AQC are active fields themselves [39, 40]. Simulations performed of bDA-QAOA in which the resource Hamiltonian is identical to the problem Hamiltonian to be solved, such that no DA steering single-qubit operations are required, indeed, showed no discernible net-negative impacts when compared to error-free QAOA.

Coherent errors occurring in bDA-QAOA with a non-problem-specific resource Hamiltonian, however, are expected to be more damaging than the errors in QAOA with an always-on problem Hamiltonian. This is due to the fact that in bDA-QAOA the always-on resource is not specific to the problem we wish to solve. These errors should therefore result in a less problem specific QAOA ansatz state which result in a worse expected approximation ratio at a given depth. Figure 7 displays the mean approximation ratio attained by the bDA-QAOA ansatz state. For high  $\alpha$  we see a regime in which, as expected, bDA-QAOA performs identically to error free QAOA. Secondly we see an intermediate regime where minor increases in the mean approximation ratio are observed. Finally, in the case of low  $\alpha$  we observe consistently worse results for bDA-QAOA, due to problem-misspecification induced by coherent DAQC errors.

## VIII. VARIATIONAL RESILIENCE OF DA-QAOA TO DA ERRORS

QAOA is a variational algorithm. It is expected that variational algorithms have better error tolerance properties due to the fact that a classical optimiser can account for systematic coherent over- or under-rotations and other systematic coherent errors [41], making variational quantum algorithms appealing candidates for NISQ quantum computing. QAOA works by finding a parameter set  $\vec{\beta}^*, \vec{\gamma}^*$  maximising  $\langle H_P \rangle_{\vec{\beta}, \vec{\gamma}}$ . However, when we change the QAOA ansatz operators to those of bDAQC, there is no clear reason why the parameters  $\vec{\beta}^*, \vec{\gamma}^*$  maximising  $\langle H_P \rangle_{\vec{\beta}, \vec{\gamma}}$  also maximise  $\langle H_P \rangle_{\vec{\beta}, \vec{\gamma}}^{\alpha, \text{DA}}$  where

$$\langle H_P \rangle_{\vec{\beta}, \vec{\gamma}}^{\alpha, \text{DA}} = \left\langle \vec{\beta}, \vec{\gamma} \left| \right. H_P \left| \vec{\beta}, \vec{\gamma} \right. \right\rangle^{\alpha, \text{DA}}. \quad (27)$$

Figure 8 suggests that this is not the case and shows that significant increase in the success probability of QAOA result from the variational freedom of the algorithm. Figure 8 should be understood to demonstrate the parameter regimes for which it makes more sense to perform a variational algorithm such as QAOA rather than a fixed gate sequence algorithm such as the quantum Fourier transform. For high  $\alpha$ , the error introduced by the scheme is negligible, and both variational algorithms and fixed sequence algorithms will perform similarly. In the middle of the plot, a dark turquoise band can be seen implying that while a non-variational algorithm will have low fidelity due to the presence of DA-induced coherent

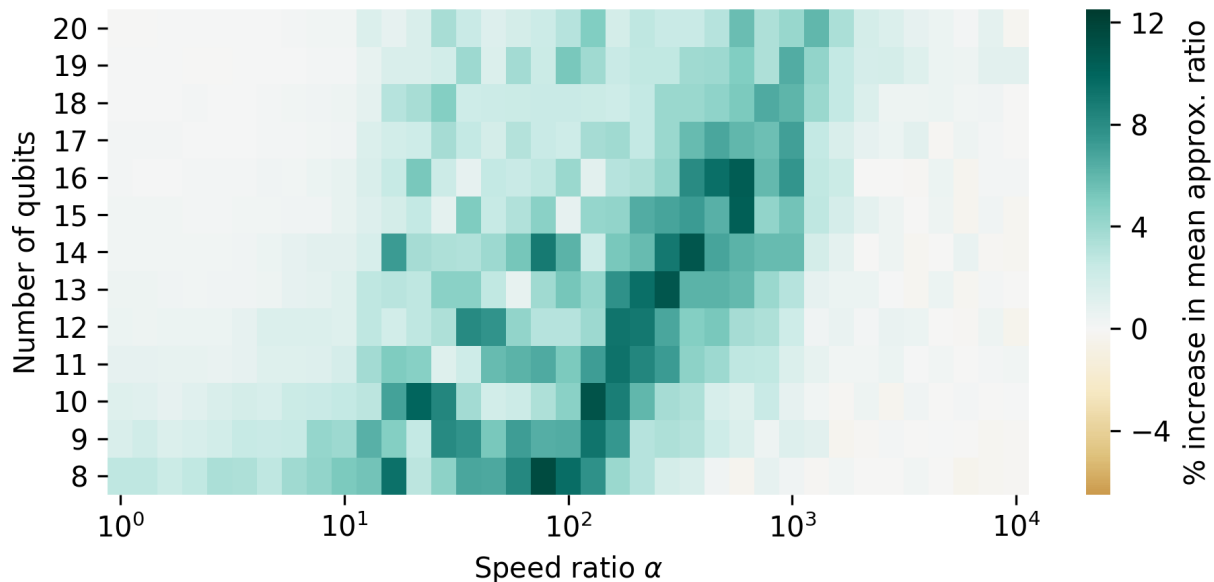


FIG. 8. The percentage difference in mean approximation ratio attained by bDA-QAOA at parameters maximising error-free QAOA and bDA-QAOA with optimised parameters, averaged over 50 randomly generated MAX-CUT problems with constant filling factor  $p_{\text{clause}} = 0.7$ . On the  $x$ -axis, the ratio  $\alpha$  of single-qubit to problem Hamiltonian term strength is seen where error-free QAOA exists in the limit as this ratio becomes infinite. Darker colours imply that for the concerned speed ratio and qubit number, the variational nature of QAOA can account for differences between bDA-QAOA and the ideal algorithm. This plot shows the benefit of using a variational algorithm such as QAOA over a non-variational algorithm in the DA context where coherent error is introduced.

errors, the variational algorithm still functions. For low enough  $\alpha$ , we enter a regime in which even the variational algorithm fails to recover any performance through altering parameters. We interpret that this lack of ability of DA-QAOA to absorb error in the low  $\alpha$  regime is a manifestation of barren plateaus in the objective function [42]. Barren plateaus are a feature discovered to occur in the optimisation landscapes of quantum neural networks. When parameterised random circuits are used as ansatz in variational algorithms, the gradient of the objective function with respect to the variational parameters is observed to become exponentially small in the number of qubits used. When  $\alpha$  reduces to a certain value, we interpret that the DA-QAOA ansatz loses specificity to the problem Hamiltonian of interest. The variational form used for optimisation no longer bears similarity to the objective function used and is, consequently, no better an ansatz than a random quantum circuit. At this point of low  $\alpha$ , we observe that the gradient of our objective function with respect to the variational parameters  $\vec{\gamma}, \vec{\beta}$  tends to become prohibitively small and the approximation ratio attained therefore varies little with differing parameters.

### IX. ANALYTICAL FIDELITY BOUNDS FOR bDA-QAOA

In this section we demonstrate that the error introduced by performing QAOA in the banded digital ana-

log paradigm in comparison to regular QAOA can be analytically bounded. In particular, we place a lower bound on the fidelity of a state that arises from a bDA-QAOA circuit in comparison to a state prepared by error free QAOA. This error consists of multiple steps, each of which is of the same nature as that occurring when Trotterizing a Hamiltonian with non-commuting terms for simulation. In the case of bDAQC induced error there are, however, two complications. Firstly, there is only a single Trotterization time-step which cannot be made arbitrarily small with the use of higher numbers of Trotter blocks. Secondly, we use Trotterization in reverse in this fidelity bound. In a usual Trotterization procedure, the simultaneous case is ‘correct’ and the digitalised version introduces error. In the digital analog scheme, however, the opposite is true. The sequential Hamiltonian is ideal and the simultaneous Hamiltonian introduces error. These differences do not affect the validity of the bound, since the bound used in this work is valid for arbitrarily large time-steps. The bound used, to our knowledge, represents the current lowest bound on Trotter error [43] and limits the size of the greatest eigenvalue of the unitary operator describing the difference between applying a two of operators sequentially instead of than simultaneously:

$$\begin{aligned} & \left\| \exp(iA/2) \exp(iB) \exp(iA/2) - \exp(i(A+B)) \right\| \\ & \leq \frac{1}{12} \left\| [[A, B], B] \right\| + \frac{1}{24} \left\| [[A, B], A] \right\|. \quad (28) \end{aligned}$$

The system Hamiltonian during time periods in which both the single-qubit operations and the resource Hamiltonian are active is

$$H_{\text{Steering}, \mu} = \alpha \sum_{m \in S_\mu} X_m + H_{\text{Resource}} \quad (29)$$

where  $S_\mu$  is the index set of  $X$  operators applied following DA time-block  $\mu$ . There are  $n(n+1)/2 + 2$  periods of time for which we apply this bound,  $n(n+1)/2$  sets of single-qubit operations following interaction blocks, one idle block and the driving block of the QAOA algorithm. We wish to compute the error resulting from using this, rather than its single-step Trotterization. Of these error effecting blocks,  $n-3$  will have four full single- $X$  rotations,  $n(n-1)/2 - (n-3) + 1$  will have two full single- $X$  rotations and one, the driver, will have  $n$  single- $X$  rotations of duration  $\beta \leq \pi$ . We can allocate  $A = tH_R$  and  $B = t\alpha \sum_{m \in S_\mu} X_m$ . Where every term in  $H_R$  consists only of Pauli- $Z$  strings. We can thus write

$$\begin{aligned} & \left\| e^{\frac{itH_R}{2}} e^{it\alpha \sum_{m \in S_\mu} X_m} e^{\frac{itH_R}{2}} - e^{it(\alpha \sum_{m \in S_\mu} X_m + H_R)} \right\| \\ & \leq \frac{\alpha^2 t^3}{12} \left\| \left[ \left[ H_R, \sum_{m \in S_\mu} X_m \right], \sum_{m \in S_\mu} X_m \right] \right\| \\ & \quad + \frac{\alpha t^3}{24} \left\| \left[ \left[ H_R, \sum_{m \in S_\mu} X_m \right], H_R \right] \right\| \quad (30) \end{aligned}$$

because every block in the DA-QAOA setting will be surrounded by resource blocks, it does not matter whether the Trotterization is symmetric or asymmetric. To calculate the first commutator, we can expand the sums and compute each individual term

$$\begin{aligned} & \sum_{m \in S_\mu} \sum_{m' \in S_\mu} \sum_{j < k} [[Z_j Z_k, X_m], X_{m'}] \\ & = \sum_{m \in S_\mu} \sum_{m' \in S_\mu} \sum_{k > m} 2[Z_m Z_k X_m, X_{m'}] \\ & \quad + \sum_{m \in S_\mu} \sum_{m' \in S_\mu} \sum_{j < m} 2[Z_j Z_m X_m, X_{m'}] \\ & = \sum_{m \in S_\mu} \sum_{m' \in S_\mu} \sum_{j \neq m} 2[Z_j Z_m X_m, X_{m'}] \\ & = \sum_{m \in S_\mu} \left( \sum_{j \neq m} 4Z_m Z_j + \sum_{m' \in S_\mu | m' \neq m} 4iY_m Y_{m'} \right). \quad (31) \end{aligned}$$

We have here assumed that the resource is homogeneous. In a given single-qubit block there will be  $s$  possible indices in the corresponding set  $S_\mu$ . As such we will have  $s(n-1)$   $Z$  strings and  $s(s-1)$   $Y$  strings. The eigenvalues of sets of terms that can be simultaneously diagonalised will add linearly. We have two orthogonal bases in which eigenvalues are added as such, the sums of which will add in quadrature. The greatest eigenvalue

of the entire sum in equation (31) can then be written  $s\sqrt{(s-1)^2 + (n-1)^2}$ . The contribution to the bound in equation (30) from this commutator can therefore be written

$$\frac{\alpha^2 t^3 s \sqrt{(s-1)^2 + (n-1)^2}}{3}. \quad (32)$$

For a homogeneous resource the commutator in the second term can be written as

$$\begin{aligned} & \sum_{m \in S_\mu} \sum_{j, j' < k, k'} [[Z_j Z_k, X_m], Z_{j'} Z_{k'}] \\ & = \sum_{m \in S_\mu} \sum_{j, j' < k, k'} 2(\delta_{jm} + \delta_{km}) [Z_j Z_k X_m, Z_{j'} Z_{k'}] \\ & = \sum_{j' < k'} \sum_{m \in S_\mu} \sum_{j \neq m} 2Z_j [Z_m X_m, Z_{j'} Z_{k'}] \\ & = \sum_{m \in S_\mu} \sum_{j \neq m} \sum_{j' \neq m} 4Z_j Z_{j'} Z_m X_m Z_m \\ & = \sum_{m \in S_\mu} \sum_{j \neq m} \sum_{j' \neq m} -4Z_j Z_{j'} X_m, \quad (33) \end{aligned}$$

where the negative sign is of no consequence. We have  $(n-1)^2$  terms per single-qubit- $X$  operator and  $s$   $X$ -operators giving  $s(n-1)^2$  strings. At worst the greatest eigenvalue of this operator sum will be equal to the number of Pauli strings. We therefore obtain a full bound of

$$\Delta_\mu = \frac{\alpha s t^3}{3} \left( \frac{(n-1)^2}{2} + \alpha \sqrt{(s-1)^2 + (n-1)^2} \right). \quad (34)$$

We wish to bound the minimum fidelity of a coherent erroneous operation caused by using bDA-QAOA

$$f_{\alpha\text{-DA-QAOA}} = \min_{\psi} \left\| \langle \psi | U_{\text{QAOA}}^\dagger U_{\alpha\text{-DA-QAOA}} | \psi \rangle \right\|^2. \quad (35)$$

If the magnitude of the greatest eigenvalue of the difference between two unitaries operators is bounded as in the Trotterization bound

$$\|U - U_\alpha\| \leq \Delta \quad (36)$$

then

$$\|U^\dagger U_\alpha - I\| \leq \Delta \quad (37)$$

which yields a bound of

$$\|e^{i|\theta|_{\max}} - 1\| \leq \Delta \quad (38)$$

where  $e^{i|\theta|_{\max}}$  is the greatest eigenvalue of  $U^\dagger U_\alpha$ , assuming the eigenvalues are small such that all angles lie on the interval  $[-\pi/2, \pi/2]$ . The greatest phase acquired under the erroneous evolution can then be related to the greatest eigenvalue bound as

$$2 \sin \left( \frac{|\theta|_{\max}}{2} \right) = \Delta, \quad \theta = 2 \sin^{-1} \left( \frac{\Delta}{2} \right) \quad (39)$$

where  $0 < \Delta < 1$ . Consider the fidelity of a state under an erroneous operator  $\hat{O} = U^\dagger U_{\text{imperfect}}$  corresponding to the time-step  $\mu$  during which a round of single-qubit-operations are performed:

$$\left\| \langle \psi | \hat{O} | \psi \rangle \right\|^2. \quad (40)$$

We can write this in the a basis diagonalising  $\hat{O}$ ,

$$\left\| \langle \psi' | \text{diag} \left( e^{i\bar{\theta}} \right) | \psi' \rangle \right\|^2 \quad (41)$$

and this fidelity is minimised when the state is an equal superposition of the most positive and most negative argument eigenstates of  $\hat{O}$ .

$$\begin{aligned} \min_{\psi'} \left\| \langle \psi' | \text{diag} \left( e^{i\bar{\theta}} \right) | \psi' \rangle \right\|^2 &= \frac{1}{4} \left\| (\langle \theta_{\max} | + \langle \theta_{\min} |) \hat{O} (|\theta_{\max}\rangle + |\theta_{\min}\rangle) \right\|^2 \\ &= \frac{1}{4} \left\| \langle \theta_{\max} | e^{i\theta_{\max}} |\theta_{\max}\rangle + \langle \theta_{\min} | e^{i\theta_{\min}} |\theta_{\min}\rangle \right\|^2 \\ &\geq \frac{1}{4} \left| e^{i|\theta|_{\max}} + e^{-i|\theta|_{\max}} \right|^2 \\ &= \cos(|\theta|_{\max})^2 \end{aligned} \quad (42)$$

So the fidelity of a single qubit block  $\mu$  is

$$f_\mu \geq \cos(|\theta|_{\max})^2, \quad (43)$$

or in terms of the bound of the greatest eigenvalue of this set of single-qubit-operations  $\Delta_\mu$

$$f_\mu \geq \cos \left( 2 \sin^{-1} \left( \frac{\Delta_\mu}{2} \right) \right)^2 \geq 1 - \Delta_\mu^2 \quad (44)$$

with equality in the limit of small  $\Delta$ . Using the subadditivity of infidelity [44] we can finally express

$$\begin{aligned} f_{\alpha\text{-DA-QAOA}} &\geq 1 - \sum_{\mu=1}^{n(n-1)/2+2} (1 - f_\mu) \\ &= 1 - \sum_{\mu=1}^{n(n-1)/2+2} \Delta_\mu^2. \end{aligned} \quad (45)$$

For one set of single-qubit-rotations, the driver, all  $X$  terms are active, giving  $s = n$ . The remaining time-blocks either have 2 or 4 single-qubit gates active determined by whether cancellations occur. No cancellations occur for  $n - 3$  blocks resulting in  $s = 4$ , with the remaining  $n(n - 1)/2 - (n - 2)$  blocks taking  $s = 2$ . The time taken to perform each block is  $t = \pi/\alpha$ . For large  $n$  we find that the speed of single-qubit gates must increase approximately as the number of qubits squared for high-fidelity with the ideal QAOA state.

## X. SENSITIVITY TO OTHER ERRORS

Next to the errors discussed in the previous sections that are imminent to the hardware simplification provided by our digital-analog approach, the algorithm is exposed to other sources of errors common to NISQ computing. As detailed error budgets of concrete hardware are currently hard to determine, we would like to qualitatively evaluate their impact on our technique.

On the one hand, single-qubit gate errors induced by decoherence measured by  $T_{1/2}$  will have full impact on this algorithm as these are repeatedly executed. Small errors of the rotation axis will also have full impact as they can be mistaken for a modified problem Hamiltonian. Errors of the rotation angle can be expected to be less critical as some of them can be accommodated in the classical optimization process. So all in all, single-qubit errors have the same if somewhat smaller impact than in a compiled gate model QAOA.

Two-qubit gates do not appear directly in our scheme thus avoiding two-qubit gate control errors as well as the additional entry points for noise through fast two-qubit control ports. However, the interaction mediated by the problem Hamiltonian can still create entangled states, which decay faster than non-entangled states. Notably, an  $n$ -qubit GHZ state dephases in a time  $T_2/n$  [45]. The precise degree of entanglement needed for a specific problem instance is currently unknown for any quantum optimization algorithms. Yet, we can summarise that the sensitivity of digital-analog QAOA to two-qubit errors is lower than the compiled version. Given a single qubit error rate, alongside the total execution time of the algorithm relative to  $T_2$ , the depth at which this algorithm can be faithfully executed could be inferred.

In this estimate we need to keep in mind whether coherent over-rotation errors have an effect different to incoherent errors. This case could occur if they interfered in a structured way. Given the randomisation effect of the problem Hamiltonian to any state, this is unlikely and we expect that their impact is faithfully represented by the measured fidelity.

## XI. CONCLUSION

The possibilities of using models of quantum computation less conventional than the standard gate based approach have not been fully considered. In this work, we show that while an alternative approach—the digital analog paradigm—might introduce errors of its own, the device complexity required to control the time evolution of the system can be reduced and errors introduced are of a nature that can be non-fatal to variational algorithms such as QAOA in certain regimes. We demonstrate that the digital analog paradigm is an ideal setting in which to do QAOA, as each problem Hamiltonian operator can be performed in a single DAQC block, that resource Hamiltonians expected from hardware can be utilised to imple-

ment QAOA Hamiltonians mitigating swapping overhead associated with mainstream approaches, and that QAOA displays error resilience beyond that of pre-programmed algorithms in the digital analog paradigm. This work presents new possibilities for the design of NISQ devices for combinatorial optimisation, bridging the gap between current devices and full, fault-tolerant quantum computers, bringing hardware closer to the point of demonstrating a quantum advantage for real-world problems.

## ACKNOWLEDGEMENTS

The authors acknowledge funding, support and computational resources from Mercedes-Benz AG, DLR, Spanish MCIU/AEI/FEDER (PGC2018-095113-B-I00), Basque Government IT986-16, the projects QMiCS (820505) and OpenSuperQ (820363) of the EU Flagship on Quantum Technologies and the EU FET Open Grant Quomorph. This work is supported by the U.S. Department of Energy, Office of Science, Office of Advanced Scientific Computing Research (ASCR) quantum algorithm teams program, under field work proposal number ERKJ333. We acknowledge useful conversations with Markus Leder, Tyler Takeshita and Tobias Stollenwerk.

- 
- [1] F. Arute, K. Arya, R. Babbush, D. Bacon, J. C. Bardin, R. Barends, R. Biswas, S. Boixo, F. G. S. L. Brandao, D. A. Buell, B. Burkett, Y. Chen, Z. Chen, B. Chiaro, R. Collins, W. Courtney, A. Dunsworth, E. Farhi, B. Foxen, A. Fowler, C. Gidney, M. Giustina, R. Graff, K. Guerin, S. Habegger, M. P. Harrigan, M. J. Hartmann, A. Ho, M. Hoffmann, T. Huang, T. S. Humble, S. V. Isakov, E. Jeffrey, Z. Jiang, D. Kafri, K. Kechedzhi, J. Kelly, P. V. Klimov, S. Knysh, A. Korotkov, F. Kostritsa, D. Landhuis, M. Lindmark, E. Lucero, D. Lyakh, S. Mandrà, J. R. McClean, M. McEwen, A. Megrant, X. Mi, K. Michielsen, M. Mohseni, J. Mutus, O. Naaman, M. Neeley, C. Neill, M. Y. Niu, E. Ostby, A. Petukhov, J. C. Platt, C. Quintana, E. G. Rieffel, P. Roushan, N. C. Rubin, D. Sank, K. J. Satzinger, V. Smelyanskiy, K. J. Sung, M. D. Trevithick, A. Vainsencher, B. Villalonga, T. White, Z. J. Yao, P. Yeh, A. Zalcman, H. Neven, and J. M. Martinis, *Nature* **574**, 505 (2019).
- [2] P. W. Shor, in *Proceedings 35th annual symposium on foundations of computer science (Ieee, 1994)* pp. 124–134.
- [3] L. K. Grover, in *Proceedings of the twenty-eighth annual ACM symposium on Theory of computing* (1996) pp. 212–219.
- [4] J. Preskill, *Quantum* **2**, 79 (2018).
- [5] A. Peruzzo, J. McClean, P. Shadbolt, M.-H. Yung, X.-Q. Zhou, P. J. Love, A. Aspuru-Guzik, and J. L. O’Brien, *Nature communications* **5**, 4213 (2014).
- [6] E. Farhi, J. Goldstone, and S. Gutmann, (2014), arXiv:1411.4028 [quant-ph].
- [7] S. Hadfield, Z. Wang, B. O’Gorman, E. G. Rieffel, D. Venturelli, and R. Biswas, *Algorithms* **12**, 34 (2019).
- [8] E. Farhi, J. Goldstone, and S. Gutmann, (2014), arXiv:1412.6062 [quant-ph].
- [9] B. Barak, A. Moitra, R. O’Donnell, P. Raghavendra, O. Regev, D. Steurer, L. Trevisan, A. Vijayaraghavan, D. Witmer, and J. Wright, (2015), arXiv:1505.03424 [cs.CC].
- [10] Z. Jiang, E. G. Rieffel, and Z. Wang, *Physical Review A* **95**, 062317 (2017).
- [11] J. S. Otterbach, R. Manenti, N. Alidoust, A. Bestwick, M. Block, B. Bloom, S. Caldwell, N. Didier, E. S. Fried, S. Hong, P. Karalekas, C. B. Osborn, A. Papageorge, E. C. Peterson, G. Prawiroatmodjo, N. Rubin, C. A. Ryan, D. Scarabelli, M. Scheer, E. A. Sete, P. Sivarajah, R. S. Smith, A. Staley, N. Tezak, W. J. Zeng, A. Hudson, B. R. Johnson, M. Reagor, M. P. da Silva, and C. Rigetti, (2017), arXiv:1712.05771 [quant-ph].
- [12] L. Lamata, A. Parra-Rodriguez, M. Sanz, and E. Solano, *Advances in Physics: X* **3**, 1457981 (2018).
- [13] A. Parra-Rodriguez, P. Lougovski, L. Lamata, E. Solano, and M. Sanz, *Physical Review A* **101**, 022305 (2020).
- [14] A. Martin, L. Lamata, E. Solano, and M. Sanz, *Physical Review Research* **2**, 013012 (2020).
- [15] I. M. Georgescu, S. Ashhab, and F. Nori, *Rev. Mod. Phys.* **86**, 153 (2014).
- [16] E. Farhi, J. Goldstone, S. Gutmann, and M. Sipser, (2000), arXiv:0001106 [quant-ph].
- [17] T. Albash and D. A. Lidar, *Reviews of Modern Physics* **90**, 015002 (2018).
- [18] J. Kempe, *Contemporary Physics* **44**, 307 (2003).
- [19] V. M. Kendon, *Philosophical Transactions of the Royal Society A: Mathematical, Physical and Engineering Sciences* **364**, 3407 (2006).
- [20] S. Lloyd, *Science*, 1073 (1996).
- [21] D. Aharonov, W. van Dam, J. Kempe, Z. Landau, S. Lloyd, and O. Regev, (2004), arXiv:0405098 [quant-ph].
- [22] A. Acín, I. Bloch, H. Buhrman, T. Calarco, C. Eichler, J. Eisert, D. Esteve, N. Gisin, S. J. Glaser, F. Jelezko, S. Kuhr, M. Lewenstein, M. F. Riedel, P. O. Schmidt, R. Thew, A. Wallraff, I. Walmsley, and F. K. Wilhelm, *New Journal of Physics* **20**, 080201 (2018).
- [23] A. Galicia, B. Ramon, E. Solano, and M. Sanz, (2019), arXiv:1912.09331 [quant-ph].
- [24] B. O’Gorman, W. J. Huggins, E. G. Rieffel, and K. B. Whaley, (2019), arXiv:1905.05118 [quant-ph].
- [25] P. K. Barkoutsos, G. Nannicini, A. Robert, I. Tavernelli, and S. Woerner, (2019), arXiv:1907.04769 [quant-ph].
- [26] S. Hadfield, (2018), arXiv:1805.03265 [quant-ph].
- [27] V. Akshay, H. Philathong, M. E. S. Morales, and J. Biamonte, (2019), arXiv:1906.11259 [quant-ph].
- [28] R. M. Karp, *Complexity of computer computations* (Springer, 1972) pp. 85–103.
- [29] C. Ballance, T. Harty, N. Linke, M. Sepiol, and D. Lucas, *Physical review letters* **117**, 060504 (2016).

- [30] N. M. Linke, D. Maslov, M. Roetteler, S. Debnath, C. Figgatt, K. A. Landsman, K. Wright, and C. Monroe, *Proceedings of the National Academy of Sciences* **114**, 3305 (2017).
- [31] P. Krantz, M. Kjaergaard, F. Yan, T. P. Orlando, S. Gustavsson, and W. D. Oliver, *Applied Physics Reviews* **6**, 021318 (2019).
- [32] P. Schauss, (2017), arXiv:1706.09014 [quant-ph].
- [33] J. P. Gaebler, T. R. Tan, Y. Lin, Y. Wan, R. Bowler, A. C. Keith, S. Glancy, K. Coakley, E. Knill, D. Leibfried, and D. J. Wineland, *Phys. Rev. Lett.* **117**, 060505 (2016).
- [34] Y. Wang, M. Um, J. Zhang, S. An, M. Lyu, J.-N. Zhang, L.-M. Duan, D. Yum, and K. Kim, *Nature Photonics* **11**, 646 (2017).
- [35] J. Zhang, G. Pagano, P. W. Hess, A. Kyprianidis, P. Becker, H. Kaplan, A. V. Gorshkov, Z.-X. Gong, and C. Monroe, *Nature* **551**, 601 (2017).
- [36] D. Porras and J. I. Cirac, *Physical review letters* **92**, 207901 (2004).
- [37] A. Pearson, A. Mishra, I. Hen, and D. A. Lidar, *NPJ Quantum Information* **5**, 1 (2019).
- [38] A. Callison, N. Chancellor, F. Mintert, and V. Kendon, *New Journal of Physics* **21**, 123022 (2019).
- [39] J. G. Morley, N. Chancellor, S. Bose, and V. Kendon, *Physical review A* **99**, 022339 (2019).
- [40] S. Muthukrishnan, T. Albash, and D. A. Lidar, (2015), arXiv:1505.01249 [quant-ph].
- [41] J. R. McClean, J. Romero, R. Babbush, and A. Aspuru-Guzik, *New Journal of Physics* **18**, 023023 (2016).
- [42] J. R. McClean, S. Boixo, V. N. Smelyanskiy, R. Babbush, and H. Neven, *Nature communications* **9**, 1 (2018).
- [43] I. D. Kivlichan, C. Gidney, D. W. Berry, N. Wiebe, J. McClean, W. Sun, Z. Jiang, N. Rubin, A. Fowler, A. Aspuru-Guzik, H. Neven, and R. Babbush, (2019), arXiv:1902.10673 [quant-ph].
- [44] M. A. Nielsen and I. Chuang, *Quantum computation and quantum information* (Cambridge University Press, 2000).
- [45] W. Dür and H. Briegel, *Physical review letters* **92**, 180403 (2004).